Applied Physics B (2024) 130:180
https://doi.org/10.1007/s00340-024-08314-w

RESEARCH

Effect of dephasing on modulation transfer in potassium

Vinay Shukla[1] · Pratanu Chakraborty[2] · Ayan Ray[1,2]

Received: 21 May 2024 / Accepted: 30 August 2024

Abstract

In this work, experimental studies on the effect of dephasing on modulation transfer are reported. Here Potassium D1 transition, i.e., ^{39}K $4S_{1/2}(F) \rightarrow 4P_{1/2}(F^{/})$, is used as the medium. The 4 S→4P connection is modified by introducing two independent lasers. The separation between ground hyperfine states $4S_{1/2}(F=2,1)$ is almost half of Doppler width (~815 MHz). Hence, the two-level connections satisfied by respective lasers are overlapping in nature. In such cases, the existing optical pumping for particular F = 1, 2→ $F^{/}$ channel influences each other. Further, the D1 transition itself is an open transition, i.e., it does not have any cyclic decay route. Hence, decay from each of the $F^{/}$=2,1 states can also influence the population in the other $F^{/}$state. Our pump-probe spectroscopy results clearly show the presence of Four Wave Mixing due to degenerate two-level and Vee (V) coupling, Electromagnetically Induced Transparency (EIT) signals due to single Lambda (Λ) and Double Λ connections. We have studied these signals as a function of dephasing, which is mainly contributed by transit time broadening for two different regimes of pump laser intensities: (i) below and (ii) above saturation intensity level of $4S_{1/2}(F) \rightarrow 4P_{1/2}(F^{/})$ transition. The pump laser is current modulated, and phase-sensitive detection is performed on the probe transmission to study modulation transfer under different values of coherent dephasing. For this purpose, the beam size of the pump laser is varied systematically. This study provides a scope to explore the modulation transfer as a function of transit time broadening, and it may find applications in photonics technology where potassium vapor is used as a medium.

1 Introduction

Pump-probe spectroscopy in alkali atoms is mainly based on conditions satisfying three basic configurations: Lambda (Λ), Vee (V) and Ladder (Ξ) [1], where Electromagnetically Induced Transparency (EIT) is commonly observed. Apart from these it is possible to construct degenerate two-level connection (DTLC) linkage. Such linkage results in phenomena like electromagnetically induced absorption (EIA) [2]. However, most experimental studies are based on systems like Rubidium and Cesium. For both these samples, the difference between ground hyperfine states is 3.03 GHz (^{85}Rb), 6.8 GHz (^{87}Rb) and 9.2 GHz (^{133}Cs) [3]. These values are much larger than the Doppler width of ~1 GHz. So, pump and probe lasers can address specific transitions separately. However, for alkali elements like ^{11}Na [3] and ^{39}K [4], the difference between ground hyperfine states is 1.7 GHz and 462 MHz. These values are close to the Doppler width value. In addition, the hyperfine level splitting of the ^{39}K D2 transition $4S_{1/2}\rightarrow 4P_{3/2}$ is much smaller than the D1 transition, i.e., $4S_{1/2}\rightarrow 4P_{1/2}$. This leads to important spectroscopic differences between saturation absorption spectroscopy (SAS) results of D1 and D2 transitions. The full-width at half-maximum (FWHM) of spontaneous decay 4P→4 S for ^{39}K transition is in the order of $\Gamma \approx 2\pi$ * 6.0 MHz [4]. This is in the order of hyperfine level splitting of the $4P_{3/2}$ level, thereby bringing in effects from neighboring transitions and significant off-resonant excitation. However, the hyperfine level spacing of $4P_{1/2}$ is much larger than Γ. So, the SAS of ^{39}K D1 can reveal the hyperfine and crossover spectra with better clarity compared to that of the D2 transition. It leads to the observation of hyperfine, crossover and ground-state crossover resonance on a single Doppler background for D1 transition. While performing the coherent pump-probe spectroscopy, a strong laser beam is passed through the sample cell either collinearly or anti-collinearly

✉ Vinay Shukla
v.shukla@vecc.gov.in

[1] Variable Energy Cyclotron Centre, A CI of Homi Bhabha National Institute, Kolkata, West Bengal 700064, India

[2] Radioactive Ion Beam Group, Variable Energy Cyclotron Centre, Kolkata, West Bengal 700064, India

Published online: 17 September 2024

with the probe laser. When the pump-probe combination is collinear, it can give rise to finer details of the coherent spectrum by exercising velocity-selective optical pumping. Wong et al. [5] reported about thirteen pump-probe spectroscopy resonances in the case of the Na vapor sample. Presence of forward near-degenerate four-wave mixing (FDFWM) and saturation in a two-level system, difference-frequency crossing and non-degenerate four-wave mixing (NDFWM) in a three-level V system, Λ type EIT and optical pumping in a three-level system, cross-transition resonance in a double Λ system and conventional optical pumping are reported in Ref. [5]. Some of these resonances tend to show sub-natural width. These ultra-narrow spectral signatures can find their application in metrology and related applications in photonics technology.

In this work, we used naturally abundant potassium vapor as the medium to conduct spectroscopy. Abundance of ^{39}K is 93.3%. The D1 transition is chosen for pump-probe laser coupling. The pump laser is relatively stronger than the probe and tuned to different frequency positions in the $4S_{1/2}(F) \rightarrow 4P_{1/2}(F')$ transition manifold. Since the difference between ground state hyperfine components ($\Delta E_{F=2\leftrightarrow1} \approx 462$ MHz) is more than half the Doppler width ($\Delta\omega_D \approx 800$ MHz [6]), it is not possible to clearly segregate the components of $F=1, 2\rightarrow F'$ through SAS. Instead, one can obtain ground state crossover resonance flanked by $F=1\rightarrow F'$ and $F=2\rightarrow F'$ hyperfine components on a large Doppler background. This type of overlapping influences the results of coherent pump-probe spectroscopy [7]. The probe laser is much weaker than the pump and only monitors the effect of coherence. Spectral features similar to that of Wong et al. [5] are observed under a pump intensity value less than the saturation intensity level of the D1 transition. However, two additional narrow transparency windows are observed when the pump laser power exceeds the saturation intensity of the same transition. We used different beam sizes of the pump laser to explore the effect of transit time broadening on the coherence in the ^{39}K D1 transition case. To use these narrow.

spectral features for metrology purposes, one needs to generate proper error signals for respective coherent features.

We modulated the pump laser frequency and detected the weak probe laser through phase-sensitive detection under different values of beam size. It effectively represents transit time broadening vs. modulation transfer for closely packed ground hyperfine levels like ^{39}K. Keeping in mind the figure 462 MHz or half of it (231 MHz), we may think of a situation where sidebands can be generated from a single laser to satisfy Λ connection and to employ the same for applications like time standard [8] or precise magnetometry [9]. Electronics-wise, this system will be much easier to implement compared to Rb or Cs standards, which require rf in the range of GHz. However, this advantage may get compromised due to the fact that the coherent feature of potassium is relatively more complicated to understand than Rb or Cs. The main reason is the small value of $\Delta E_{F=2\leftrightarrow1}$. Hence, it is of great importance to put the modulation transfer into competition with coherent dephasing to optimize the error signal.

2 Energy level diagram and experimental schematic

The relevant level schematic of the ^{39}K D1 transition is shown in Fig. 1. A Potassium vapor cell (without buffer gas; dimensions 25 mm×75 mm) is used as a sample cell. The cell is heated to 60ºC to attain sufficient vapor pressure ~ 10^{-6} mbar [4] required for absorption spectroscopy. Two single-mode tunable external cavity diode lasers (cf. Figure 1) connecting $4S_{1/2} \xrightarrow[770nm]{} 4P_{1/2}$ are used for pump-probe spectroscopy. The frequency of the pump field (ω_{pu}) is fixed at specific points by monitoring the SAS of the D1 line. The relatively weaker laser (ω_{pr}) is scanned to probe the signals obtained due to coherence between two lasers co-propagating through the sample cell. A wavemeter and a Fabry-Perot etalon are used to provide a coarse estimate of wavelengths and the single-mode scanning of the laser. Both pump and probe lasers are linearly polarized but orthogonal to each other. After mixing them on a Polarizing Cube Beam Splitter (PCBS), the beams are passed through a λ/4 plate. So, the pump-probe combination satisfies the σ^+-σ^- polarization combination.

The transmitted beams are again passed through a λ/4 plate and then separated using another PCBS. The probe beam is detected with a photodiode. Two beam expanders are used in the pump and probe laser paths. While the probe is held at a constant narrow beam size, the pump beam size is varied. This is done to put the existing coherence into competition with dephasing, principally governed by transit time broadening. For modulation purposes, the current of the pump laser is modulated with a small sinusoidal voltage at 5 kHz frequency. The probe laser response is detected with a lock-in amplifier. It may be noted that the ^{39}K D1 transition is open. So atoms can decay to either of the ground state hyperfine levels. Figure 1 (A) → (F) shows that the atoms can get stored in the degenerate magnetic sublevels (m_f) dark states indicated by bold lines. These magnetic sublevels belong to ground hyperfine state components. The six configurations shown in Fig. 1 for σ^+-σ pump-probe polarization combination are made considering pure two-level laser excitation. The situation is complex in practice because the relatively narrow energy gap $\Delta E_{F=2\leftrightarrow1}$ makes it

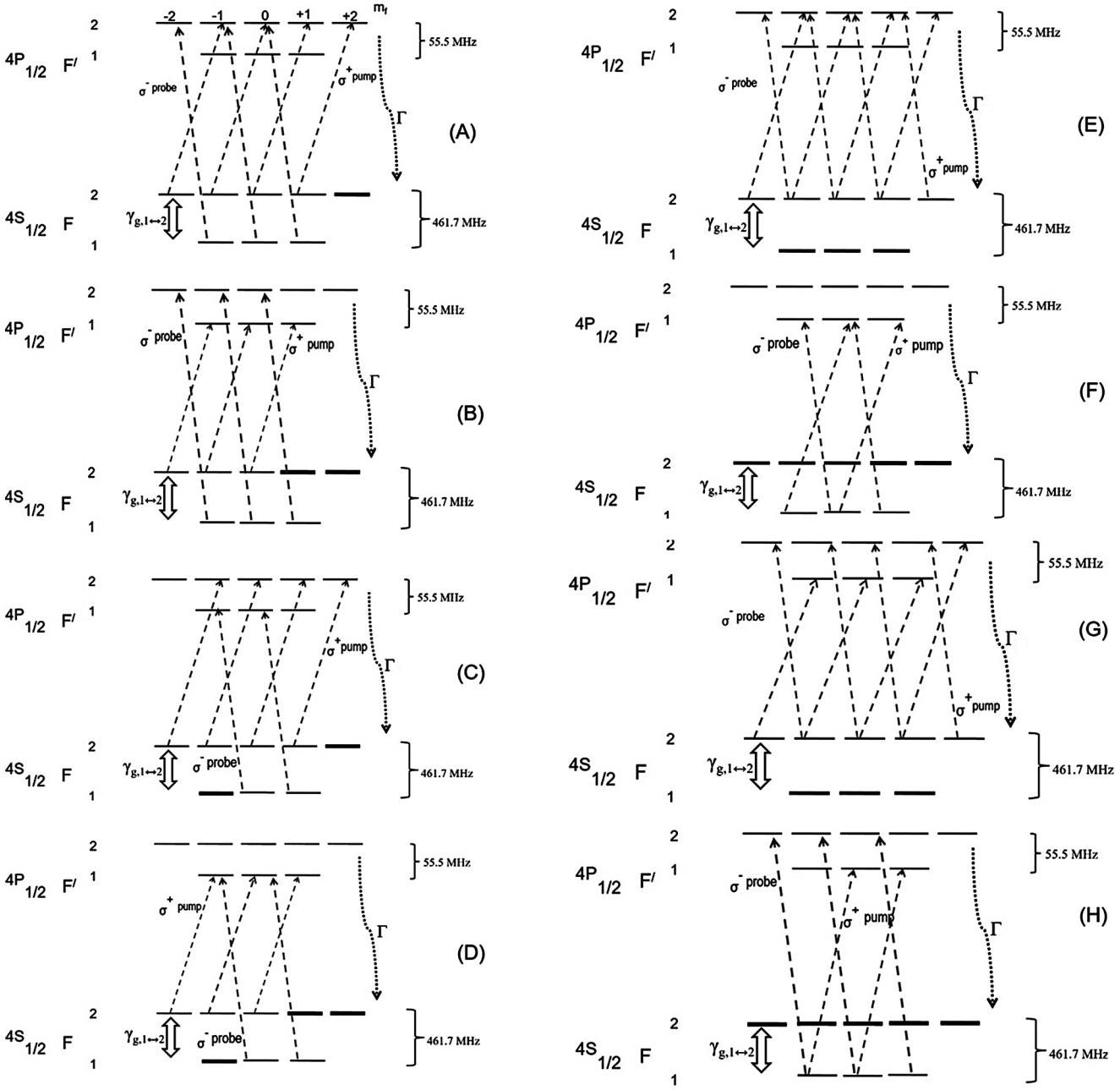

Fig. 1 Level scheme in $4S_{1/2} \xrightarrow[770nm]{} 4P_{1/2}$ transition of ^{39}K atom with their respective degenerate Zeeman sublevels (m_f). Dephasing between ground-state hyperfine components: $\gamma_{g,1\leftrightarrow 2}$ is governed by the transit time broadening (without buffer gas; negligible collisional effect as mean free path > > wavelength of laser). Spontaneous decay $\Gamma \approx 2\pi$ * 6.0 MHz. The two-photon resonance condition is $\Delta\omega_{pu} + \Delta\omega_{pr} \approx 0$. The $4P_{1/2}$ level has a lifetime $\tau_{4P1/2} \approx 26.37$ns. Combinations (**A**)→(**D** show possible Λ connections, whereas (**E** and (**F** show possible degenerate two-level linkages under 'F' level basis. Further, (**G**) and (**H** show two V-type combinations out of four possible connections. Bold lines show Zeeman sublevels acting as a population dark state during the excitation-decay process

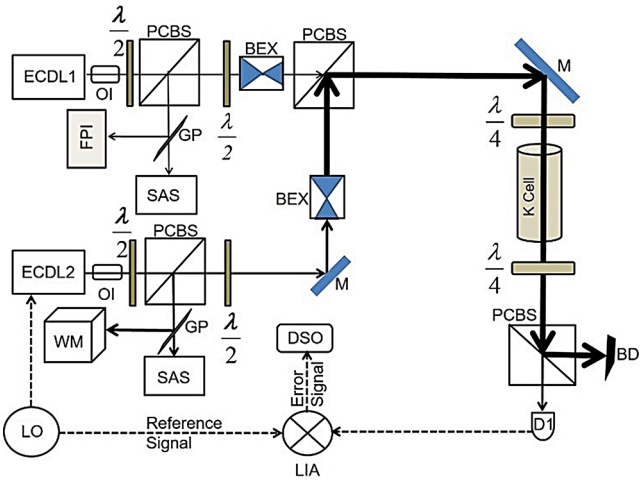

Fig. 2 Schematic of the experimental arrangement. ECDL: external cavity diode laser, BEX: Beam Expander, BS: beam splitter, PCBS: polarizing cubic beam splitter, OI: optical isolator, M: mirror, D: photodetector, λ/2: half-wave plate, λ/4: quarter-wave plate, WM: wave-meter, FPI: Fabry-Perot Interferometer, DSO: digital storage oscilloscope, LIA: lock-in amplifier, LO: local oscillator, SAS: saturation absorption spectroscopy set up, GP: glass plate, BD: beam dump. ECDL1(2) are probe(pump) Toptica DL100 lasers with linewidth < 1 MHz, elliptical beam 1:3 mm

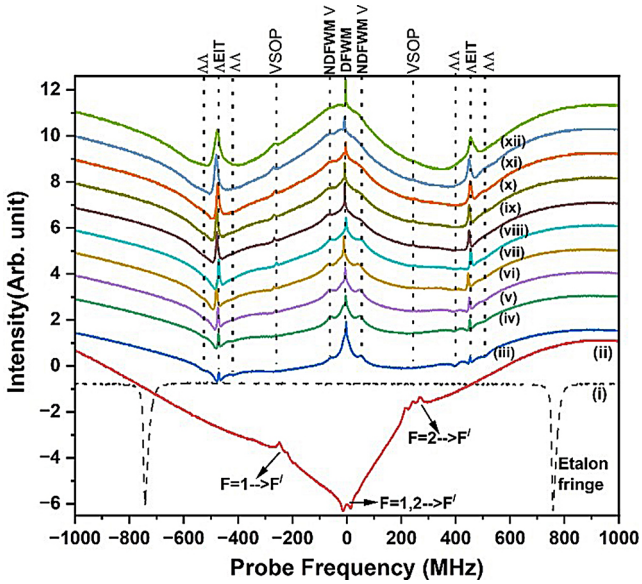

Fig. 3 Recording of the probe transmission as a function of frequency after coherent interaction within the K vapor cell. Here (i) shows a recording of the Etalon fringe with FSR 1.5 GHz, and (ii) shows the saturation absorption signal of the probe laser for ^{39}K atom. Further (iii)→(xii) show the spectra under pump power values of 0.3, 0.5, 1.0, 1.5, 2.0, 3.2, 4.2, 6.15, 11.0, 22.5 mW. DFWM: degenerate four-wave mixing due to two-level connection; NDFWM V: non-degenerate four-wave mixing under V linkage; Λ EIT: Electromagnetically Induced Transparency in Λ coupling. Apart from them, two dips due to ΛΛ (double lambda) connection are observed around each Λ EIT up to 2mW pump laser power, which is marginally larger than the saturation intensity [4]. Velocity selective optical pumping (VSOP) signals appear as mirror images on both sides of the DFWM signal peak at positions: F = 1→F′ and F = 2→F′

impossible for lasers to maintain two-level approximations during excitation. In a simplistic manner, one can assume that the lasers satisfy an admixture of all these configurations while scanned through the ^{39}K D1 hyperfine domain. Earlier, Wong et al. [5] reported pump-probe resonances in ^{23}Na D1 transition where the energy gap between ground hyperfine levels (1.7 GHz for Na) is in the order of Doppler width. We used the experimental result of Ref. [5] to understand the mechanisms behind pump-probe resonances within the ^{39}K D1 transition.

3 Results and discussions

The current experimental configuration (cf. Figure 2) has circularly polarized (σ^+ - σ^-) pump and probe beams co-propagating through the K vapor cell at 60°C. Co-propagating geometry is highly velocity selective. Hence relatively narrow velocity group of atoms take part in pump-probe resonance compared to counter propagation configuration. An additional degree of selectivity is provided by σ^+ - σ^- polarization combination.

In the current experiment Fig. 3 shows the spectra of pump-probe resonances as a function of pump laser power, while probe laser power is held constant at 20μW. Both pump and probe laser beam sizes are the same, i.e., 1:1. Here, ω_{pu} is fixed at ground state crossover resonance (F = 1, 2→F′) and ω_{pr} is scanned. Further the pump laser is tuned under free running condition by changing the piezo voltage. Since the readings are taken within ~1 s the recorded spectrum is limited by the laser linewidth only.

(i) **DFWM**: The spectra of DFWM (see Fig. 3) result from degenerate FWM in a near two-level system. It shows a peak of sub-natural width (~2.5 MHz) appearing on a relatively broader lineshape (FWHM ~ 30 MHz). Contribution of linewidth from two independent lasers is < 2 MHz.

In this case, two pump photons are absorbed in exchange for generating one idler photon and the emission of one probe photon. Since the ^{39}K D1 transition is an open two-level transition, the spontaneous decay rate Γ augments the decay of atoms to a reservoir that is not directly connected to the excitation-decay cycle (see Fig. 1E, F). The atom can only return back to the cycle with the help of dephasing, i.e. $\gamma_{g,1\leftrightarrow 2}$, the sub-natural width of the peak stems from the fact $\Gamma >> \gamma_{g,1\leftrightarrow 2}$. The broader peak emanates from the saturation effect in a Doppler-broadened medium. The effect of power broadening is clearly seen in Fig. 2 (iii) → (xii).

(ii) **NDFWM and difference frequency crossing**: There are two more broad peaks that arise at ~55.5 MHz (spacing between F′=2, 1, i.e.$\Delta E_{F'=2,1}$) away from the DFWM signal. These results are obtained when it $\Delta E_{F'=2,1} \approx |\omega_{pu} - \omega_{pr}|$ is satisfied. Considering ω_{pu} to be resonant with ground hyperfine state crossover resonance, i.e., F = 1,2→F′, we can think of a situation where the set of transitions F = 1 → F′=1,2 and F = 2 → F′=1,2 are simultaneously satisfied. Also, the ground state population is re-distributed between F = 1 and 2 levels. This double resonance contributes significantly to probe absorption for the velocity group of atoms ~$\Delta E_{F'=2,1}$. Figure 1G, H show two extreme cases of the V system where two-level approximation is assumed for each excitation arm. It may be noted that two more such V combinations ($F' = 1 \xleftarrow{\sigma^- probe} F = 2 \xrightarrow{\sigma^+ pump} F' = 2$ and $F' = 2 \xleftarrow{\sigma^- probe} F = 1 \xrightarrow{\sigma^+ pump} F' = 1$) are also possible. For systems like ^{39}K D1 transition, such a distinct V connection is not possible. Instead, a set of transitions satisfying V connections play their role. It creates a situation of difference frequency crossing, which resonates with only one velocity group of atoms. For a scanning ω_{pu}, this resonance is satisfied for two positions ± 55.5 MHz about 0-th position. However, the FWM associated with this complex process is non-degenerate (NDFWM) in nature. The idler field is doubly resonant, and peaks are observed when (ω_{pu} - ω_{pr}) matches$\Delta E_{F'=2,1}$. Contribution from difference frequency crossing gets obscured with increment in pump power, and the effect of NDFWM becomes dominant.

(iii) **ΛEIT, ΛΛ and VSOP**: It is seen in Fig. 3 that EIT windows appear at values of ± 462.7 MHz from the position of F = 1,2→F′. At this position (ω_{pu} - ω_{pr}) becomes equal to the separation between F = 1,2. In such cases, destructive quantum interference occurs between excitation pathways connecting F→F′. Figure 1A→D shows all possible Λ connections for σ^+-σ pump-probe combination under two-level excitation approximation. For such schemes, atoms are stored in dark states and get thermalized again due to dephasing $\gamma_{g,1\leftrightarrow 2}$. Such EIT linewidth is principally limited by dephasing. For pump power up to 1mW, the EIT linewidth varies from ~2.5 MHz to 6 MHz. When pump power exceeds saturation intensity, the linewidth gets power broadened.

For relatively low pump power (0.3→1.5mW), we can notice two symmetrical dips at ~55 MHz (≈ $\Delta E_{F'=2,1}$) away from Λ EIT peak. These pair of dips are broad (≤ 30 MHz). In addition to these two transmission dips, another broad dip centered on the EIT feature exists. These are products of difference frequency crossing due to optical pumping in addition to saturation. A similar type of resonance can be seen in a ΛΛ system. No EIT peak is observed. In such cases, the stronger pump and the weak probe lasers are resonant with different sets of transitions. The pump field drives the population to an excited state, and the atoms decay to both ground levels. Since probe power is weaker, the population accumulates at the ground level of the probe transition, thereby giving rise to the probe absorption dips. These dips get obscured with an increase in pump power due to an increased level of optical pumping.

In addition to this, optical pumping in hot atomic gas – quasi-monochromatic laser interaction leads to redistribution of population in degenerate Zeeman sublevels. This situation leads to velocity selective optical pumping (VSOP) resonances. Their presence is detected at ± 232MHz {≈ $1/2(\Delta E_{F=2\leftrightarrow 1})$} at pump power values above the saturation intensity. The situation may be qualitatively understood as follows: the atoms excited to the excited state from one lower state may decay back to another lower state for an open system. So, the atoms may be transferred to the other level by velocity-selective optical pumping (VSOP). This uncoupled lower state may, in principle, lead to reduced absorption. This is because some velocity groups of atoms cannot take part in the absorption. For higher pump power, this velocity-selective optical pumping becomes prominent, and the transparency window becomes more important. However, this absorption transparency is different from the EIT window.

(iv) **Dephasing vs. modulation transfer**: Spectra in Fig. 3 show two signals of sub-natural line widths: Λ EIT and DFWM in a two-level system. Both of them depend on the value of $\gamma_{g,1\leftrightarrow 2}$working in the system. Since the system is open and $\Gamma >> \gamma_{g,1\leftrightarrow 2}$, the decay of atoms to an additional reservoir (in this case, uncoupled ground state component) is inevitable. In the case of Λ EIT, the least linewidth achievable is$\gamma_{g,1\leftrightarrow 2}$. On the other hand, the DFWM peak resides on a broad peak, which is a product of saturation in a two-level Doppler broadened system. The width of the DFWM peak depends on the decay rate of the ground level out of the two-level subsystems. Processes like thermal redistribution and diffusion of atoms into and out of the interaction zone are dominant contributors in the present experiment. Figure 4 provides a closer look at the spectroscopic results obtained under variable pump beam size.

The transit time broadening is proportional to (v/d), where **v** is the most probable velocity of the atom, and **d** is the diameter of the beam. Hence, variation in beam size changes the dephasing. Since the probe beam size is held constant, the

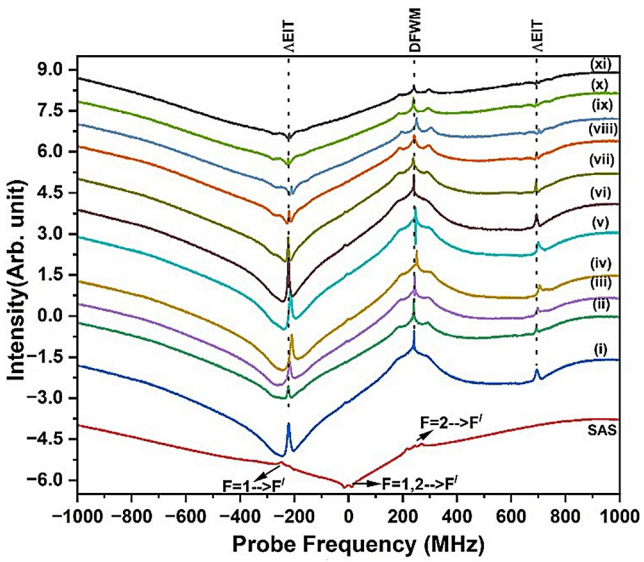

Fig. 4 Recording of the probe transmission as a function of frequency after coherent interaction within the K vapor cell. Here (i) → (xi) show recording of the probe absorption signal of probe laser for ^{39}K atom under pump beam sizes: (1/5)X, (1/4)X, (1/3)X, (1/2.5)X, (1/2)X, (1/1.5)X, 1X, 1.5X, 2X, 2.5X, 3X. The probe beam size is fixed at (1/3)X; ω_{pu} is fixed at the vicinity of F = 2→F′ of SAS spectra. The DFWM peak and Λ EIT signals are shifted accordingly. The probe (pump) power kept at 20μW (2mW)

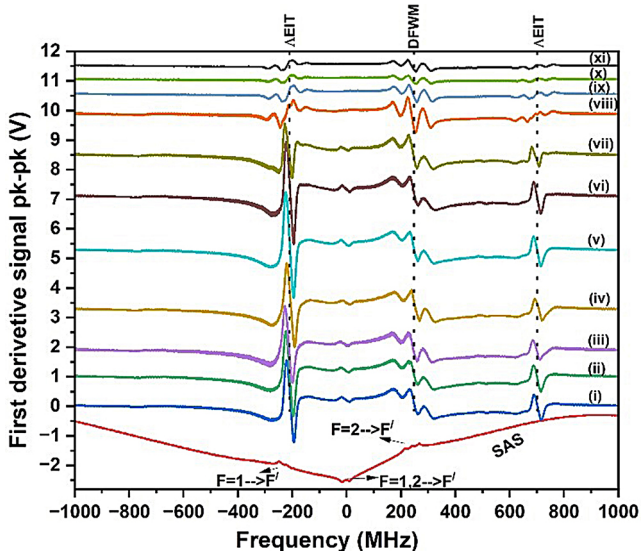

Fig. 5 Recording of the first derivative signal of pump-probe laser spectra (under probe scan) after coherent interaction within the K vapor cell. Here (i) → (xi) show recording of the lock-in detection of probe absorption signal for ^{39}K atom under pump beam sizes: (1/5)X, (1/4)X, (1/3)X, (1/2.5)X, (1/2)X, (1/1.5)X, 1X, 1.5X, 2X, 2.5X, 3X. The probe beam size is fixed at (1/3)X; ω_{pu} is fixed at the vicinity of F = 2→F′ of SAS spectra. The DFWM peak and Λ EIT signals are shifted accordingly. The probe (pump) power kept at 20μW (2mW)

dephasing is solely varied by pump beam size. The intensity of the pump beam varies from ~ 1 W/cm^2 to 0.1 W/cm^2. So, all the case studies were made above the saturation intensity level (of D2 transition) of 1.75mW/cm^2 [4]. With the highest value of dephasing {(1/5)X beam size}, coherent features like DFWM and EIT become prominent. The DFWM is observed to reside on a dome-like structure, resulting from the saturation effect. At this stage, the linewidth of EIT is in the order of Γ. The lowest value of dephasing (5X beam size) results in the near obscuring of coherent features. Moderate value of dephasing {Fig. 5 (iv) → (vii)} show DFWM peak with a reduced level of saturation effect and EITs with sub-natural linewidth. These can be effectively used as frequency discriminators.

Coherent spectroscopy of ^{39}K D1 presents a versatile spectrum where destructive quantum interference and degenerate four-wave mixing are the mechanisms producing sub-natural linewidth. Similar kind of result for ^{41}K was reported earlier [10]. It may be noted that current experiment utilises σ$^+$- σ$^-$ polarization combination. However the spectra obtained is similar to that presented in Ref. 5 where linear-perpendicular-linear (lin. ⊥ lin.) polarization is used. Under both lin. ⊥ lin. and $\sigma^+-\sigma^-$ polarization combinations the population tend to be distributed in zeeman sublevels of the ground state hyperfine components. This can be detected by a probe beam monitoring the absorption spectra in a pump induced coherently prepared medium. Crosstalk between pump-probe combination is possible due to ensuing coherence in the medium [13, 14]. In effect $\sigma^+-\sigma^-$ combination can result into highest degree of crosstalk. This fact was pointed in earlier study on open transition [16]. For system like ^{39}K atom where $\Delta E_{F=2\leftrightarrow1} < \Delta\omega_D$ is satisfied, the transitions F = 1, 2 → F′=2, 1 swap with each other. Here the $\sigma^+-\sigma^-$ combination offers a limited degree of selection in the zeeman sublevel (m_f) basis for transition pathways. The DFWM signal arises from the coherent contribution of different zeeman sublevels pairs excited by the field. Due to spontaneous decay no zeeman sublevel pair is closed [17] D1 transition manifold.

A simple experimental study is conducted to find out the efficacy of these signals as frequency discriminators. The relatively stronger pump laser is current modulated at 5 kHz, and the probe laser transmitted through the K cell is detected through a lock-in amplifier (Fig. 5). Demodulation of the probe resonance is done at 5 kHz to obtain the first derivative signal. Frequency spacing between the extreme points of the linear part of the derivative signal provides a measure of the linewidth of spectrum.

The most striking feature of Fig. 5 is the phase change of the first derivative of the ΛEIT feature starting from a pump beam size of 1.5X. This shows that as the value of transit time broadening gets weaker, the ΛΛ dips start to affect the

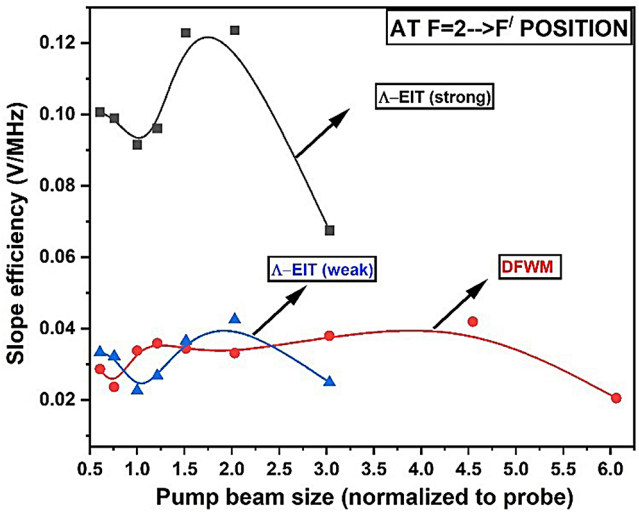

Fig. 6 Slope efficiency (1st derivative signal) vs. pump beam size data. The strong EIT appears at the position of $F=1\rightarrow F'$ SAS signal position, and the weak EIT is at detuned condition + 462.7 MHz from $F=2\rightarrow F'$ position (cf. Figures 4 and 5). The DFWM shows relative immunity to transit time broadening (dephasing) compared to EIT

ΛEIT signal. At a further lower value of transit time broadening, the EIT signal is obscured. For the first derivative of the DFWM signal, such phase change is not noticed. The difference frequency crossing does not affect the DFWM idler field. For a pump beam size of (1/2)X → 1.5X, the first derivative signals with a good (S/N) ratio are obtained. It may be noted that the width of the first derivative signals of EIT and DFWM are in the range of ~ 3Γ. This happened because we have directly modulated the pump laser drive current, which adds up to the linewidth of the two interacting lasers due to coherence-induced modulation transfer. This difficulty can be avoided if an external modulator is used [17] or high-frequency current modulation is used to generate sidebands with a single laser. At present, we do not have that facility. However, the results presented in Fig. 5 act as indicators of the ongoing competition between dephasing vs. modulation transfer. Slope efficiency (V/MHz) vs. pump beam size shows the behavior of two different types of discriminators as a function of transit time broadening. Figure 6 illustrates the results of the experimental study.

The ΛEIT signal is suitable to be used as a frequency discriminator as its slope efficiency is higher than DFWM. However, this is only possible for a limited zone of pump: probe beam combination. In a sense, it shows the sensitivity of the EIT signal to dephasing. Modulation transfer also follows the same nature. Apart from this zone, the ΛEIT signal is affected by the dips caused by ΛΛ connection. However, the DFWM signal and related modulation transfer are apparently immune to dephasing. Though EIT-induced modulation transfer is higher than that of DFWM, the optimization of the experimental layout is more stringent in the case of EIT. This indicates that modulation transfer vs. dephasing shows a trade-off between EIT and DFWM.

4 Conclusion

In this paper, we focused on experimentally studying an alkali atom system (^{39}K D1 transition) from the perspective of pump-probe-induced coherent spectroscopy. The system is intrinsically different from other alkali atoms (like Rb, Cs) as the separation between ground hyperfine states of ^{39}K is less than the Doppler width. Further, the system is open. So, it is not possible to couple any two energy levels distinctly by laser excitation. Instead, the coupling will affect other energy levels and can exhibit spectra exhibiting Λ EIT, ΛΛ dips, degenerate four-wave mixing (DFWM), V-type crossings, two-level saturation etc. Prominent spectral features are analyzed following the work reported by Wong et al. [5]. Among them, DFWM and EIT show sub-natural widths for certain pump-probe combinations. The separation between ground hyperfine state $4S_{1/2}$ of ^{39} K is 461.7 MHz, which is easily achievable by a readily available function generator. It leaves open the possibility of constructing portable photonic devices like atomic clocks, magnetometers, etc., with relatively simpler electronic layouts. It may not require high-end radio frequency electronics. However, this prospect can only be utilized if one studies sub-natural resonances in coherent pump-probe spectroscopy. For this purpose, we generated the first derivative discriminator signal of DFWM and Λ EIT by direct modulation of the pump laser and studied the slope efficiency as a function of different pump beam sizes for a fixed geometry of the probe beam. Since the K cell is at 60°C and without any buffer gas, we can neglect the effect of velocity-changing collisions. In such cases, the dephasing between ground state components is governed by transit time broadening. The results show that the DFWM can be used as a discriminator almost immune to dephasing but with lesser efficient modulation transfer than Λ EIT. On the other hand, the Λ EIT may show a higher degree of modulation transfer, but it is highly sensitive to dephasing. It may be noted that the present experimental study is carried out at a higher saturation intensity regime. However, the below saturation intensity investigation may leave more interesting aspects to study, such as an exhibition of the transfer of coherence and its manifestation to EIA-like features besides DFWM and EIT.

Author contributions Author 1(Vinay Shukla) made substantial contributions to the work's conception and design, as well as to the acquisition, analysis, drafting and interpretation of data.Author 2(Pratanu Chakraborty): made contributions to the acquisition, drafting and analysis of the data.Author 3 (Ayan Ray) contributed to the conception or design of the work, acquisition, drafting and the interpretation of data.

Funding Open access funding provided by Department of Atomic Energy.

Data availability Data underlying the results presented in this paper are not publicly available at this time but may be obtained from the authors upon reasonable request.

Declarations

Competing interests The authors declare no competing interests.

References

1. J. David, S. Fulton, R.R. Shepherd, B.D. Moseley, Sinclair, M.H. Dunn, Continuous-wave electromagnetically induced transparency: a comparison of V, Λ, and cascade systems. Phys. Rev. A **52**, 2302 (1995)
2. A. Lipsich, S. Barreiro, A.M. Akulshin, A. Lezama, Absorption spectra of driven degenerate two-level atomic systems. Phys. Rev. A **61**, 053803 (2000)
3. https://steck.us/alkalidata
4. T.G. Tiecke, *Properties of Potassium*, van der Waals-Zeeman Institute, University of Amsterdam, The Netherlands v1.0February (2010)
5. V. Wong, R.W. Boyd, C.R. Jr. Stroud, R.S. Bennink, A.M. Marino, Thirteen pump-probe resonances of the sodium D1 line. Phys. Rev. A **68**, 012502 (2003)
6. R.K. Hanley, P.D. Gregory, I.G. Hughes, S.L. Cornish, Absolute absorption on the potassium D lines: theory and experiment. J. Phys. B: Mol. Opt. Phys. **48**, 195004 (2015)
7. S. Gozzini, A. Fioretti, A. Lucchesini, L. Marmugi, C. Marinelli, S. Tsvetkov, S. Gateva, S. Cartaleva, Tunable and polarization-controlled high-contrast bright and dark coherent resonances in potassium. Opt. Lett. **42**, 2930 (2017)
8. J.S. Guzman, A. Wojciechowski, J.E. Stalnaker, K. Tsigutkin, V.V. Yashchuk, D. Budker, Nonlinear magneto-optical rotation and Zeeman and hyperfine relaxation of potassium atoms in a paraffin-coated cell. Phys. Rev. A **74**, 053415 (2006)
9. D.A. Keder, D.W. Prescott, A.W. Conovaloff, K.L. Sauer, An unshielded radio-frequency atomic magnetometer with sub-femtotesla sensitivity. AIP Adv. **4**, 127159 (2014)
10. W. Wang, A.M. Akulshin, M. Ohtsu, Pump-probe Spectroscopy in Potassium using an AlGaAs laser and the second harmonic generation of an InGaAsP laser for frequency stabilization and linking. IEEE Photon Technol. Lett. **6**, 95 (1994)
11. A.W. Brown, M. Xiao, Modulation transfer in an electromagnetically induced transparency system. Phys. Rev. A **70**, 053830 (2004)
12. Y.B. Kale, A. Ray, R. D'Souza, Q.V. Lawande, B.N. Jagatap, Atomic frequency offset locking in a Λ type three-level Doppler broadened Cs system. Appl. Phys. B **100**, 505 (2010)
13. Y.B. Kale, A. Ray, Q.V. Lawande, B.N. Jagatap, Coherent spectroscopy of a Λ atomic system and its prospective application to tunable frequency offset locking. Phys. Scr. **84**, 035401 (2011)
14. L. Mudarikwa, K. Pahwa, J. Goldwin, Sub-doppler modulation spectroscopy of potassium for laser stabilization. J. Phys. B Mol. Opt. Phys. **45**, 065002 (2012)
15. S. Khan, A.-. Hassan, H.R. Noh, J.T. Kim, Theoretical and experimental study of modulation transfer spectroscopy fornon-cycling transitions of rb D1 lines. J. Quant. Spectr. Rad Trans. **322**, 109037 (2024)
16. A. Lezama, G.C. Cardoso, J.W.R. Tabosa, Polarization dependence of four-wave mixing in a degenerate two-level system. Phys. Rev. A **63**, 013805 (2000)
17. A.D. Innes, P. Majumder, H.R. Noh, S.L. Cornish, Modulation transfer spectroscopy of the D1 transition of potassium: theory and experiment. J. Phys. B: Mol. Opt. Phys. **57**, 075401 (2024)